Differential cross sections for K^-p elastic scattering from 1.4 to 1.9 GeV/c*

K. Abe,† B. A. Barnett, J. H. Goldman,‡ A. T. Laasanen,§ and P. H. Steinberg
University of Maryland, College Park, Maryland 20742

G. J. Marmer, D. R. Moffett, and E. F. Parker
Argonne National Laboratory, Argonne, Illinois 60439

(Received 5 March 1975)

We report here the results from an experiment to obtain differential cross sections for K^-p elastic scattering in the laboratory momentum region from 1.4 to 1.9 GeV/c. These data span the region of a bump in the K^-p total cross section at an energy of 2.05 GeV. Approximately 20000 elastic events were obtained at each of four momenta with an angular coverage of $0.9 \geq \cos\theta_{\text{c.m.}} \geq -0.9$. The data are intended to aid in phase-shift analyses of the resonances causing the bump in the total cross section and to study dip structures at constant values of the Mandelstam variables t and u.

I. INTRODUCTION

The K^-p system has been studied extensively during the past decade in the resonance region up to 2.5 GeV/c. Many Λ and Σ resonances have been found in this region as illustrated in Fig. 1 which shows the total K^-p cross section[1] versus K^- laboratory momentum. The cumulative evidence for these resonances is quite varied, however. Some of them are well established while others are quite uncertain.[2] Perhaps the most powerful method for establishing these resonances has been phase-shift analyses of data from formation types of experiments $K^-p \to (\Lambda, \Sigma)$. The agreement among the various analyses[3] is reasonably good below 1.2 GeV/c, but very little is known about the resonances around the bump near energy 2.05 GeV. Of the eight suspected resonances in this region only two are well established.[2]

The data from K^-p experiments have also been interesting because of dip structures observed in the elastic differential cross sections. For ex-

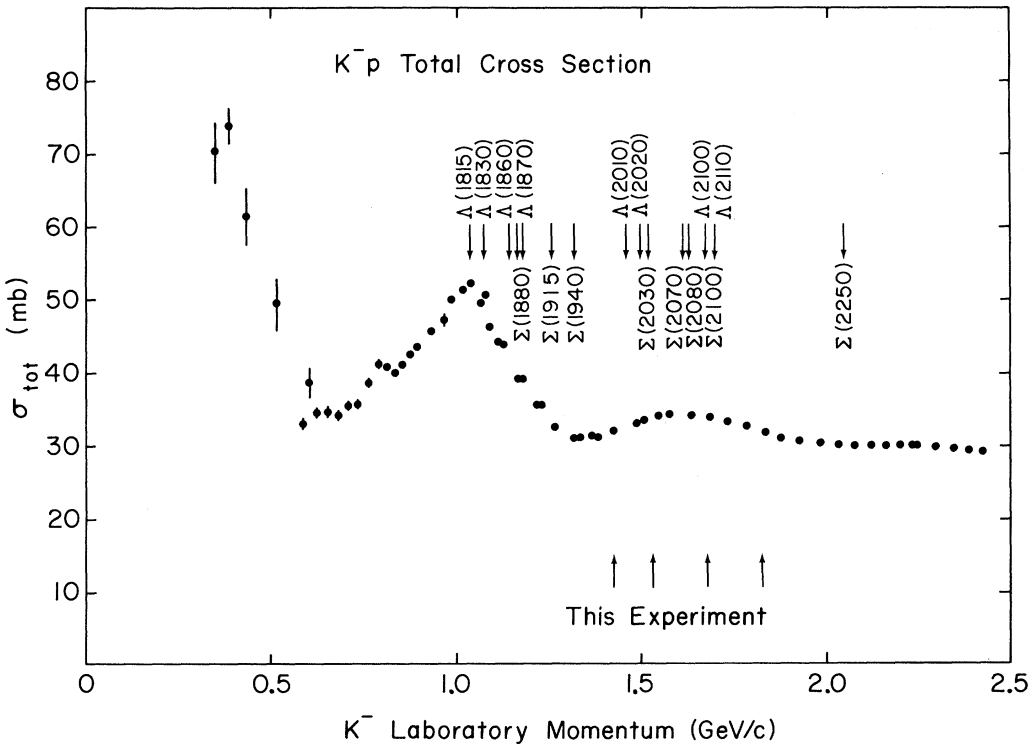

FIG. 1. K^-p total cross section versus momentum.

ample, Daum *et al.*[4] found evidence for a dip in the backward region at a fixed value of the Mandelstam variable $u \approx -0.32$ (GeV/c)^2. A dip at a constant u value would normally be explained by a u-channel particle exchange, but in the case of K^-p such an exchange would have to be an exotic baryon, i.e., a $qqqq\bar{q}$ state in quark model notation. Such a particle could also show up as an s-channel resonance in K^+p scattering. The existence of an exotic resonance of this kind is somewhat controversial,[5] having been observed in K^+p phase-shift analyses done by some groups and not by others. An alternative explanation to such a dip structure has been suggested by Odorico[6] in terms of the Veneziano model. He showed that dips at constant u might be generated without requiring the exchange of an exotic baryon.

This article describes a measurement of the elastic K^-p differential cross section over an angular region of $0.9 \geq \cos\theta_{\text{c.m.}} \geq -0.9$ at four momenta in the region of the 2.0 GeV bump as indicated by the arrows in Fig. 1. These data were taken as the final part of an experiment performed at the Argonne National Laboratory Zero Gradient Synchrotron (ZGS) which measured the elastic differential cross section in K^+p,[7,8] π^+p,[9,10] and pp (see Ref. 11) scattering from 0.8 to 2.3 GeV/c. The experiment utilized a multiplaned wire-spark-chamber system for final-state particle detection which reduced systematic uncertainties and allowed the measurements to be carried out to an increased statistical precision. It also achieved an absolute normalization to within 4%, whereas most previous data in this region were normalized to total cross section results via the optical theorem. Thus, besides acquiring improved data for phase-shift analyses, the experiment also provides a measurement of the total elastic cross section and a determination of the cross section at zero scattering angle.

The remainder of this paper is divided into two sections as follows. Section II provides a brief description of the experimental method and analysis with more complete descriptions being given in other publications.[7,9,12] Section III presents the final results of the experiment and discusses their physical significance.

II. EXPERIMENTAL METHOD AND ANALYSIS

The experiment was performed in a partially separated K^- beam at the Argonne ZGS. The purity of the beam was somewhat less than 1% in our momentum region, so that the kaons had to be identified electronically from a substantial background. This was done using time-of-flight and two Čerenkov counters, one of which was a gas threshold type[13] while the other was a liquid differential type.[14] Conservative checks of the pion rejection efficiencies for these counters during each beam tuning gave 99.9% for each counter. This gave a π^- contamination in our final K^- signal on the order of 0.1%. The beam normally delivered about 600 K^-'s per gated beam spill in a momentum bite of ±1.5% around a central momentum known to 0.3%.

The experimental apparatus itself is shown schematically in Fig. 2. After passing through an upstream scintillation counter for time-of-flight measurement, the K^- passed through the two

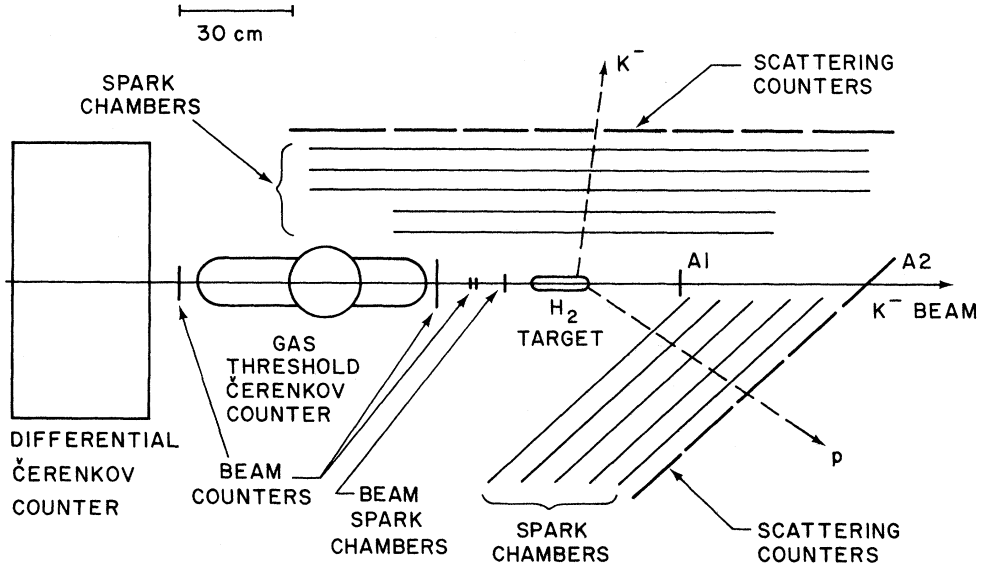

FIG. 2. Experimental setup.

Čerenkov counters, several other beam counters, and eventually entered a cylindrical liquid hydrogen target having a length of 6 in and a diameter of 1.5 in. If it did not scatter from a proton in this hydrogen, the K^- continued undeflected into two veto counters, A_1 and A_2. If the K^- did scatter in the hydrogen it traveled to the left (right) while the struck proton traveled to the right (left), where each passed through five planes of two-dimensional, magnetostrictive read out, wire spark chambers, and a plane of scintillation counters. The spark chambers were fired, and data was read into an online computer, whenever a beam K^- disappeared and a particle was detected in each of these scintillation counter banks.

The desired elastic scattering events were identified by comparison of the particle directions with those expected from elastic kinematics. Up to four sparks were recorded for each coordinate of each chamber, and lines were made of three or more sparks. The forward-going particle was normally detected in the spark chamber system on the right side of the beam, i.e., the set which is at 45° to the beam, and the backward-going particle was detected in the left-hand system. The kinematical selection of elastic events allowed a unique identification of the particles at all center-of-mass scattering angles except in a small region called the "region of kinematic ambiguity." This is the region near the center-of-mass scattering angle where both particles have the same momentum and angle relative to the initial beam direction. For the K^- beam momenta in this experiment it occurred at $\cos\theta_{\text{c.m.}} \approx 0.13$. We could accept the data point at which both particles had the same scattering angle, since there was no ambiguity about the center-of-mass angle in this case, but data in a small region on each side were discarded. After the reconstructed events were cut to assure a vertex in the liquid hydrogen target, the events were sorted into $\cos\theta_{\text{c.m.}}$ bins. The differential cross sections were obtained from the bin populations by applying corrections for the geometric efficiency, inelastic background, kaon decay, particle rescattering, target length, hydrogen density, K^- beam attenuation, accidental triggers, high-voltage pulse efficiency, and track recognition efficiency of the spark chambers. The uncertainties in the incident flux, the hydrogen density, and the target length contributed to the overall normalization uncertainty, while the other factors contributed to the point-to-point statistical uncertainty. The contributions to the statistical errors are included in the errors assigned to the data points quoted later in this report. The normalization uncertainty arising from the above factors was ±1%.

This normalization uncertainty has been increased because of particle background effects upon the spark chamber efficiency determination. The efficiency of each spark chamber was continually monitored during the experiment by means of the track reconstruction. Since there were five chambers in each of the final state detection banks, while only three chambers were required for track reconstruction, the efficiency of each chamber could be calculated from the data. This could even be done as a function of particle position in the chamber, and no positional dependence was found. The efficiencies were generally in the 90% to 98% region, so that the over-all detection efficiency should have been well over 99.5% if the inefficiencies were uncorrelated. Checks between the number of tracks missing one spark versus the number missing two sparks showed only a small amount of correlation in the inefficiencies.

A detailed examination of the data, however, suggested the existence of correlations between the chambers beyond that indicated by these studies. During the experiment the data taking was divided into runs of five to eight hours duration. Approximately ten of these runs were obtained for each momentum. The consistency between these data sets was checked carefully. No variation was found in the shapes of the angular distributions in these runs in either the K^-p data or in the π^+p, K^+p, or pp data. The normalizations, however, were found to vary from run to run in a way that was correlated to the instantaneous beam rate and the over-all spark-chamber detection efficiency calculated by assuming no correlations in the individual chamber efficiencies. This variation was not due to the exclusion of events with extra tracks, a low multispark spark-chamber efficiency, or to an insufficient number of spark scalars. It was clear, however, that the high beam rate, and the associated high backgrounds in our experimental area, increased the failures of the spark chambers in a way that was uncorrectable by a method which assumed only the small degree of chamber correlation indicated by the number of tracks missing two sparks compared to one spark. The data were corrected for this effect by finding the dependence of the elastic cross section on the calculated chamber efficiency and extrapolating linearly to 100% efficiency. The result of this extrapolation was in substantial agreement with the result obtained by a similar linear extrapolation to zero instantaneous beam rate. All subsets of data were normalized to this value of σ_{elastic}. The procedure was followed at each momentum point, and, as a result, the normalization was changed by 2% at 1.530 GeV/c, 5% at 1.680 GeV/c, and 6% at 1.815 GeV/c from that

obtained in the highest efficiency run. No change was necessary at 1.423 GeV/c. The uncertainty in the extrapolation was about 4%, so this was combined with the uncertainty due to the kaon flux, hydrogen density, and target length to obtain the final normalization uncertainty.

III. EXPERIMENTAL RESULTS AND CONCLUSIONS

The final values of the differential cross sections obtained in this experiment are given in Table I and displayed graphically in Fig. 3. The statistical error for each point is quoted in the table and shown on the graph. There is also a normalization uncertainty of 4% for the data at 1.423, 1.530, and 1.680 GeV/c and 5% at 1.815 GeV/c. The solid lines drawn through the data are the results of a Legendre-polynomial fit, which is described below. The cross sections at all four momenta have similar shapes, namely a sharp forward diffractive peak followed alternately by two dips and two peaks.

A. Parameterization of the cross section

The differential cross sections have been parameterized by means of the Legendre-polynomial expansion

$$\frac{d\sigma}{d\Omega} = \frac{1}{k^2} \sum_{l=0}^{L} A_l P_l(\cos\theta_{\text{c.m.}}) .$$

The order of the fitting, given by L, was determined by examining the stability of the A_l's versus L. The value of $L = 8$ was chosen from this procedure for all four momenta. The sets of coeffi-

TABLE I. K^-p differential cross sections at 1.423, 1.530, 1.680, and 1.815 GeV/c.

$\cos\theta_{\text{c.m}}$ \ Momentum	1.423 GeV/c	1.530 GeV/c	1.680 GeV/c	1.815 GeV/c
0.875	3.083 ± 0.084	3.169 ± 0.063	3.414 ± 0.082	3.013 ± 0.085
0.825	2.107 ± 0.064	1.945 ± 0.043	2.060 ± 0.060	1.794 ± 0.064
0.775	1.580 ± 0.056	1.278 ± 0.034	1.263 ± 0.047	1.193 ± 0.051
0.725	1.150 ± 0.047	0.804 ± 0.028	0.706 ± 0.035	0.628 ± 0.038
0.675	0.958 ± 0.042	0.509 ± 0.020	0.485 ± 0.029	0.397 ± 0.030
0.625	0.671 ± 0.036	0.395 ± 0.019	0.265 ± 0.021	0.232 ± 0.024
0.575	0.521 ± 0.032	0.219 ± 0.015	0.152 ± 0.019	0.150 ± 0.020
0.525	0.372 ± 0.025	0.173 ± 0.014	0.122 ± 0.017	0.121 ± 0.019
0.475	0.313 ± 0.023	0.146 ± 0.010	0.091 ± 0.013	0.097 ± 0.018
0.425	0.295 ± 0.025	0.094 ± 0.011	0.118 ± 0.013	0.084 ± 0.021
0.375	0.231 ± 0.022	0.084 ± 0.010	0.089 ± 0.015	0.119 ± 0.024
0.325	0.186 ± 0.015	0.075 ± 0.011	0.110 ± 0.020	0.088 ± 0.020
0.275	0.165 ± 0.014	0.066 ± 0.009		0.114 ± 0.015
0.225	0.156 ± 0.018	0.072 ± 0.010		
0.125	0.157 ± 0.014	0.084 ± 0.011	0.121 ± 0.013	0.112 ± 0.015
0.025	0.158 ± 0.015			
−0.025	0.162 ± 0.014			0.122 ± 0.018
−0.075	0.142 ± 0.013	0.133 ± 0.013	0.132 ± 0.021	0.097 ± 0.014
−0.125	0.166 ± 0.014	0.146 ± 0.013	0.137 ± 0.017	0.142 ± 0.015
−0.175	0.178 ± 0.019	0.147 ± 0.014	0.105 ± 0.017	0.133 ± 0.020
−0.225	0.168 ± 0.014	0.147 ± 0.013	0.175 ± 0.019	0.116 ± 0.020
−0.275	0.151 ± 0.021	0.185 ± 0.014	0.123 ± 0.017	0.112 ± 0.018
−0.325	0.185 ± 0.020	0.149 ± 0.013	0.162 ± 0.019	0.105 ± 0.020
−0.375	0.124 ± 0.016	0.146 ± 0.013	0.139 ± 0.017	0.099 ± 0.019
−0.425	0.148 ± 0.018	0.125 ± 0.011	0.138 ± 0.017	0.143 ± 0.020
−0.475	0.155 ± 0.019	0.135 ± 0.011	0.099 ± 0.016	0.074 ± 0.018
−0.525	0.175 ± 0.019	0.148 ± 0.013	0.118 ± 0.017	0.083 ± 0.018
−0.575	0.185 ± 0.019	0.161 ± 0.013	0.138 ± 0.017	0.065 ± 0.015
−0.625	0.274 ± 0.023	0.171 ± 0.013	0.147 ± 0.017	0.065 ± 0.016
−0.675	0.277 ± 0.023	0.178 ± 0.014	0.120 ± 0.017	0.092 ± 0.019
−0.725	0.336 ± 0.028	0.230 ± 0.016	0.138 ± 0.021	0.074 ± 0.016
−0.775	0.396 ± 0.028	0.273 ± 0.016	0.163 ± 0.020	0.075 ± 0.016
−0.825	0.440 ± 0.029	0.307 ± 0.019	0.184 ± 0.017	0.136 ± 0.019
−0.875	0.415 ± 0.028	0.370 ± 0.020	0.215 ± 0.020	0.099 ± 0.015

cients and the confidence levels of the fits thus obtained are given in Table II and graphed relative to A_0 in Fig. 4. These are seen to exhibit a smooth dependence upon momentum. The lines drawn through the points in the figure are merely to guide the eye.

The total elastic cross section was obtained by integrating the differential cross section over the entire solid angle using the results of the Legendre-polynomial fit. This gives $\sigma_{el} = 4\pi A_0/k^2$. The values for σ_{el} thus obtained are listed in Table II. The errors quoted include the normalization uncertainties discussed earlier and the statistical uncertainties of the fitting procedure. Figure 5 shows our values of σ_{el} along with the values obtained from other experiments[4, 15] plotted versus momentum. This shows that our lower two points are in agreement with other experiments but that the points of both Daum *et al.* and Litchfield *et al.* are significantly higher than ours at 1.680 and 1.815 GeV/c. Neither of these experiments had an absolute normalization, but instead were normalized to the optical theorem by extrapolating to zero scattering angle using the Legendre-polynomial fit. If we treat our data in the same fashion as they treated theirs our normalization would increase by up to 15%.

The fact that using a Legendre-polynomial fit and the optical theorem causes our value of σ_{el} to rise should not be taken to mean that our data with the absolute normalization as assigned is in violation of the optical theorem. It instead shows the need for care in using the optical theorem for normalization. Figure 6 shows our forward data fitted to an exponential, i.e.,

$$\frac{d\sigma}{dt}(t) = \left.\frac{d\sigma}{dt}\right|_{t=0} e^{Bt}$$

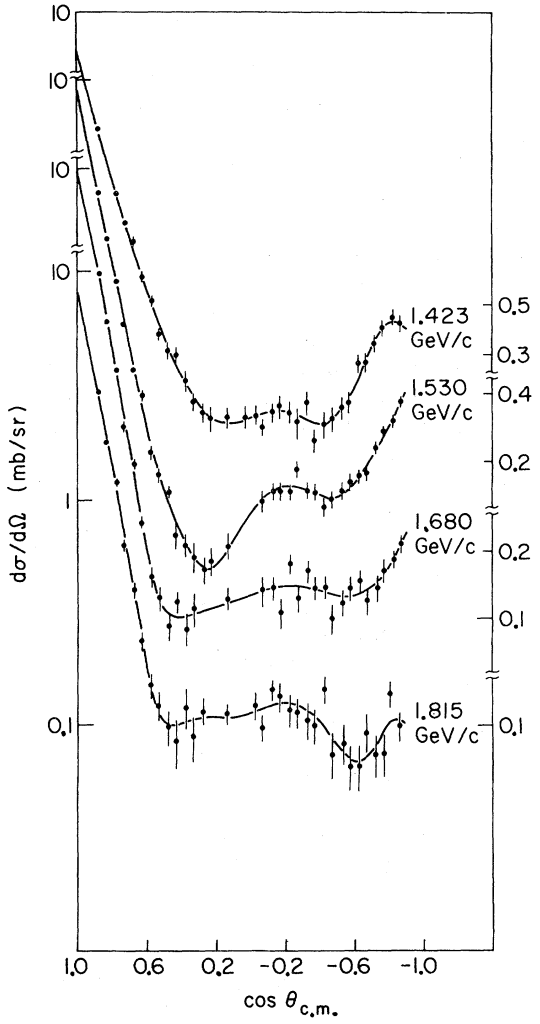

FIG. 3. Differential cross section versus $\cos\theta_{c.m.}$.

TABLE II. Legendre-polynomial expansion coefficients, confidence levels, and elastic cross sections.

	1.423 GeV/c	1.530 GeV/c	1.680 GeV/c	1.815 GeV/c
A_0	0.779 ± 0.020	0.831 ± 0.015	0.945 ± 0.021	0.888 ± 0.021
A_1/A_0	1.733 ± 0.082	1.856 ± 0.057	2.075 ± 0.068	2.251 ± 0.083
A_2/A_0	2.393 ± 0.139	2.946 ± 0.101	3.022 ± 0.118	2.996 ± 0.132
A_3/A_0	2.004 ± 0.126	2.639 ± 0.091	2.963 ± 0.112	3.131 ± 0.132
A_4/A_0	1.325 ± 0.158	2.367 ± 0.115	2.625 ± 0.138	2.606 ± 0.152
A_5/A_0	0.976 ± 0.111	1.441 ± 0.074	1.686 ± 0.092	1.784 ± 0.108
A_6/A_0	0.227 ± 0.130	0.903 ± 0.085	1.009 ± 0.104	0.928 ± 0.113
A_7/A_0	0.322 ± 0.063	0.483 ± 0.040	0.424 ± 0.053	0.466 ± 0.060
A_8/A_0	0.016 ± 0.066	0.182 ± 0.045	0.130 ± 0.057	0.050 ± 0.059
C. L.	61%	40%	24%	42%
σ_{el}	8.42 ± 0.40 mb	815 ± 0.36 mb	8.19 ± 0.37 mb	6.95 ± 0.38 mb

in the forward-most direction. The t region of this fit was determined by examining the stability of the $(d\sigma/dt)|_{t=0}$ and B parameters as the maximum $|t|$ was increased. The arrows indicate the optical-theorem limit. The extrapolated values of $(d\sigma/dt)|_{t=0}$, given the normalization uncertainty, are in agreement with or higher than the minimum value set by the optical limit. It is noteworthy, relative to the earlier comments about σ_{el}, that the two higher momentum points are further above the optical-theorem limit than the lower two points. The Legendre-polynomial expansions can be used to find extrapolated values of $(d\sigma/dt)|_{t=0}$, and these are given in Table III along with the results of the exponential fit. It is obvious from the table that the Legendre-polynomial fit produces a substantially smaller value of $(d\sigma/dt)|_{t=0}$ than does the exponential fit.

The validity of our normalization can also be supported by comparison to other forward cross section data. We display the slope parameter B versus momentum in Fig. 7 along with the results of Baillon *et al.*,[16] who measured $d\sigma/dt$ in the very small $|t|$ region. The agreement between these results indicates that the slope does not change between $t=0$ and the t region of our data. In Fig. 8 we display our values of $(d\sigma/dt)|_{t=0}$. The hatched curve in this figure represents the cross section we would predict from Baillon's results. This curve was generated by taking

$$\left.\frac{d\sigma}{dt}\right|_{t=0} = \frac{1}{16\pi\hbar^2}\,\sigma_{\text{tot}}{}^2(1+\alpha^2)$$

using Baillon's values of α, the ratio of the real to imaginary parts of the forward scattering am-

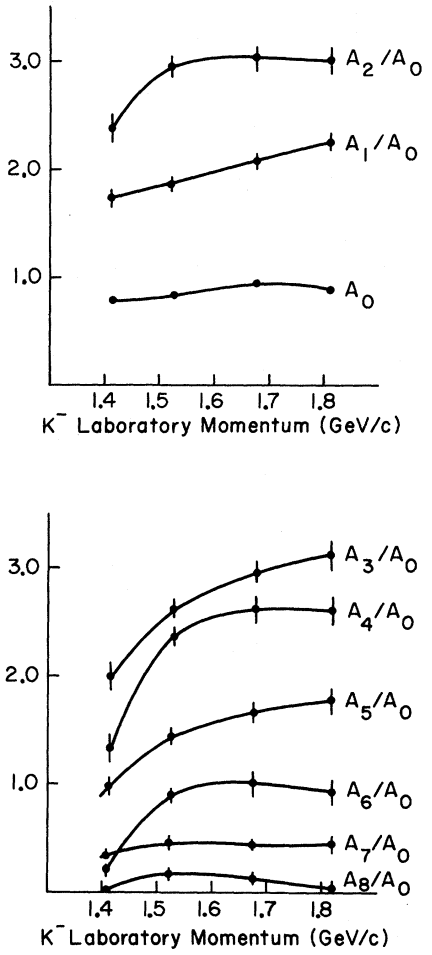

FIG. 4. Legendre-polynomial coefficients.

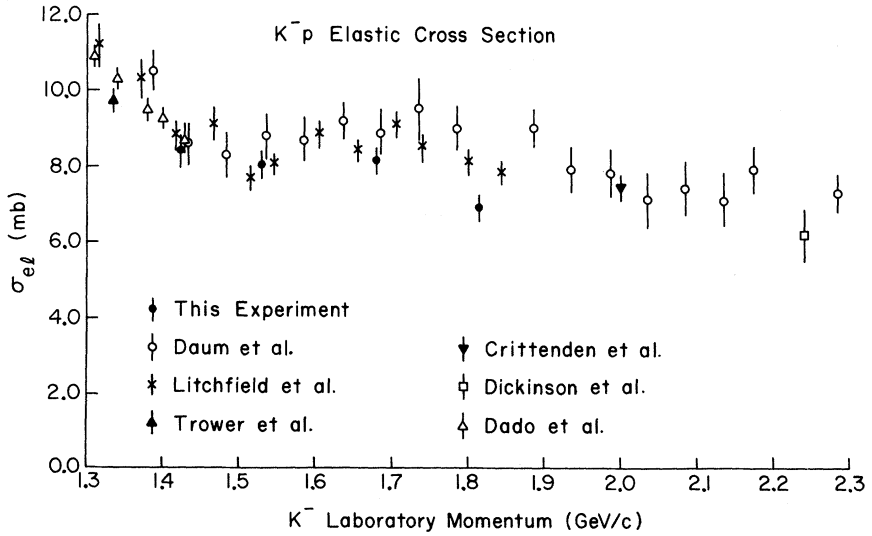

FIG. 5. K^-p elastic cross section versus momentum.

plitude, and σ_{tot} from Gilmore *et al.*[1] and Cool *et al.*[1] Baillon *et al.* claim to have a normalization accuracy of ±1%, so that the comparison shown in Fig. 8 would indicate that our normalization is either correct within the assigned errors or possibly high in the region of our disagreement with Daum *et al.* and Litchfield *et al.*

B. Dip structures in the differential cross section

The differential cross section measured by Daum *et al.*[4] displayed evidence of two dips, one at a constant value of t and one at a constant value of u. Our data are plotted in terms of $d\sigma/dt$ and $d\sigma/du$ in Figs. 9 and 10, where the solid lines are the results of the Legendre-polynomial fit. These figures clearly show both of the dips, the first at $t \approx -0.7$ (GeV/c) and the second at $u \approx -0.4$ (GeV/c).

The presence of dips at constant values of t or u are normally explained in terms of the properties of particles exchanged in that channel. This makes the dip at constant u very interesting because a single particle exchange in this channel would have to be an exotic baryon with a quark structure of "$qqqq\bar{q}$" and quantum numbers of $S=1$, $B=1$, and $Q=2$. Evidence for such a particle has been sought through phase-shift analyses in the s channel of K^+p scattering with controversial results. The most recent analysis of Arndt *et al.*[5] claims to find such a resonance with $M=1787$ MeV and $\Gamma=200$ MeV. Its elasticity, however, is very small, $x \approx 0.1$, so it is not clear that its effects in K^-p backward scattering would be large enough to account for the u-channel dip which has been observed.

An alternative explanation of the u-channel dip has been offered by Odorico[6] through use of the Veneziano model. The scattering amplitude in this model contains the term

$$\frac{\Gamma(1-\alpha(s))\,\Gamma(1-\alpha(t))}{\Gamma(2-\alpha(s)-\alpha(t))} ,$$

where $\Gamma(x)$ is a gamma function and α is the Regge trajectory in the s or t channel. Given certain

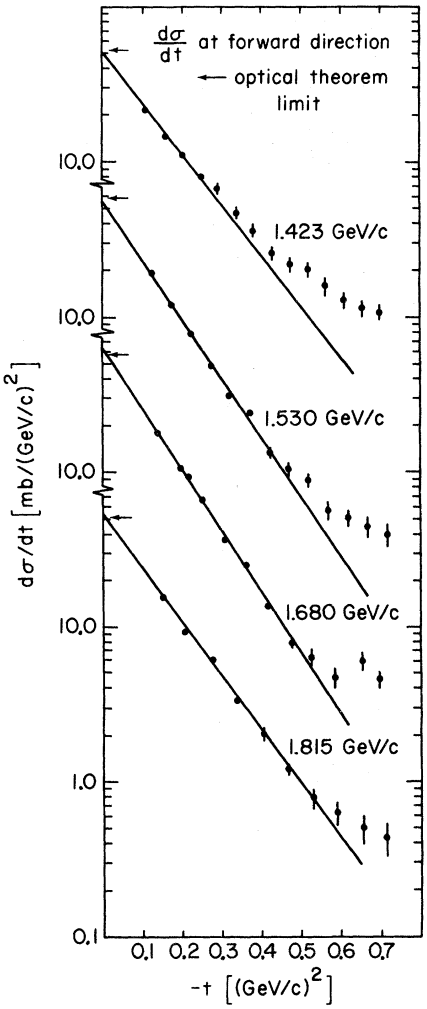

FIG. 6. Exponential fits to $d\sigma/dt$ for small $|t|$.

assumptions about the behavior of the α's, the denominator can be rewritten as

$$\Gamma(2-\alpha(s)-\alpha(t)) = \Gamma(u_0+\alpha' u) .$$

This means that the Veneziano amplitude contains a family of zeros caused by the poles in the denominator at values of u such that $(u_0+\alpha' u)$ is a

TABLE III. Results of the exponential fit to $d\sigma/dt$ for small $|t|$ and comparison to $d\sigma/dt|_{t=0}$ from Legendre-polynomial expansion.

Beam momentum (GeV/c)	Cutoff $\lvert t\rvert$ in exponential fit [(GeV/c)^2]	Exponential $\left.\frac{d\sigma}{dt}\right\rvert_{t=0}$ $\left(\frac{\text{mb}}{(\text{GeV}/c)^2}\right)$	B[(GeV/c)$^{-2}$]	$\left.\frac{d\sigma}{dt}\right\rvert_{t=0}$ $\left(\frac{\text{mb}}{(\text{GeV}/c)^2}\right)$
1.423	0.20	49.46±2.00	7.50±0.26	46.6±4.4
1.530	0.35	60.05±2.36	9.05±0.21	56.6±3.6
1.680	0.40	66.74±2.69	8.92±0.18	54.4±3.8
1.815	0.40	53.59±2.70	8.07±0.22	42.4±3.2

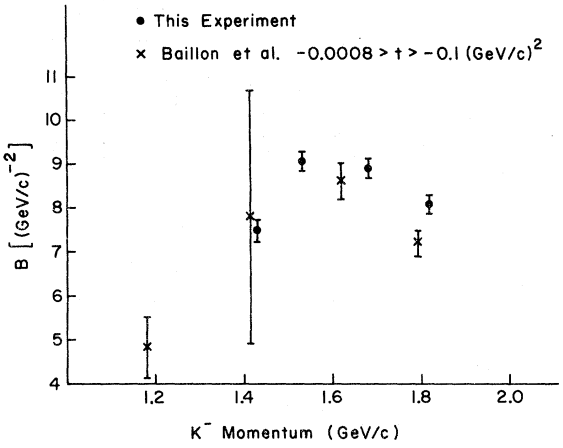

FIG. 7. Slope parameters from exponential fit to $d\sigma/dt$ for small $|t|$.

negative integer. Since the real scattering amplitude from this model could contain several terms like this, a zero in one of them could be hidden by the effects of the others. Nevertheless, this process does provide a means of producing dips at a constant value of u without requiring the existence of an exotic baryon. Another ramification of this model, however, is that dips at other values of u should exist. If $\alpha' \approx 1$, the spacing of these dips would be 1 $(\mathrm{GeV}/c)^2$, which would predict another dip in K^-p scattering at $u \approx -1.4$ $(\mathrm{GeV}/c)^2$. No significant evidence exists in our

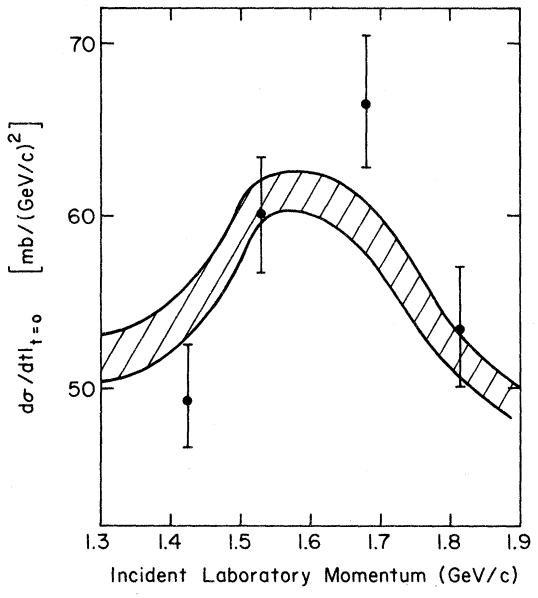

FIG. 8. Forward cross sections, $d\sigma/dt|_{t=0}$, compared to calculated results using the total cross section and ratio of real to imaginary part of the forward scattering amplitude from Ref. 1 and 16.

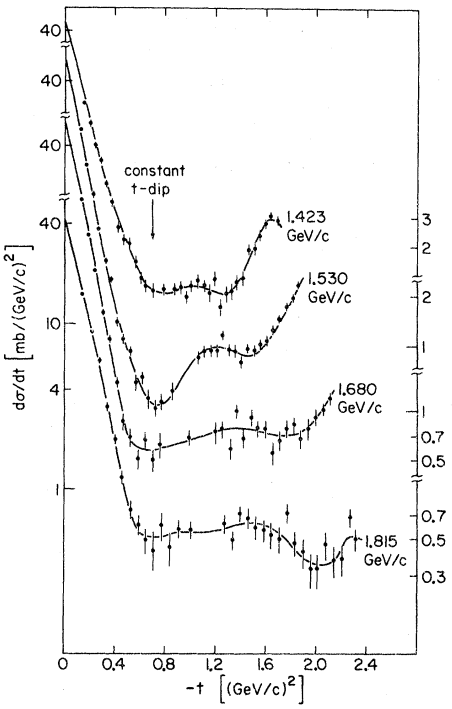

FIG. 9. $d\sigma/dt$ versus t showing evidence for dip at $t \approx -0.7$ $(\mathrm{GeV}/c)^2$.

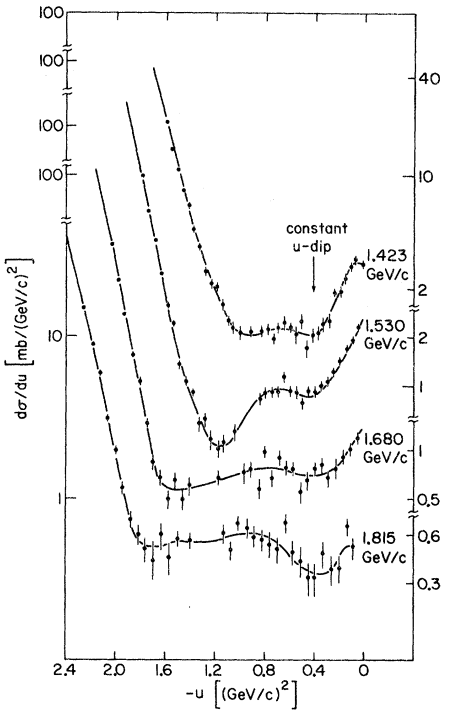

FIG. 10. $d\sigma/dt$ versus u showing evidence for dip at $u \approx -0.4$ $(\mathrm{GeV}/c)^2$.

results to substantiate a dip at this value of u. Our data is certainly not precise enough to rule out such an effect, however, so that a more careful search is probably warranted.

ACKNOWLEDGMENTS

We would like to thank the staff of the Argonne National Laboratory for their most valuable assistance. We are especially grateful to our beam physicist, Dr. Irwin Spirn, our project coordinator Dr. Russ Klem, and our engineer, Mr. Chester Brzegory.

We are also thankful to the technical staff at the University of Maryland for their help, especially during the construction phase of the experiment.

---

*Work supported by the U. S. Atomic Energy Commission.

†Present address: Department of Physics, Rutgers University, New Brunswick, New Jersey 08903.

‡Present address: Department of Physics, New York University, New York, New York 10003.

§Present address: Department of Physics, Purdue University, Lafayette, Indiana 47907.

[1]D. V. Bugg, R. S. Gilmore, K. M. Knight, D. C. Salter, G. H. Stafford, E. L. N. Wilson, J. D. Davies, J. D. Dowell, P. M. Hattersley, R. J. Homer, A. W. O'Dell, A. A. Carter, R. J. Tapper, and K. F. Riley, Phys. Rev. 168, 1466 (1968); R. L. Cool, G. Giacomelli, T. F. Kycia, B. A. Leontic, K. K. Li, A. Lundby, and J. Teiger, Phys. Rev. Lett. 16, 1228 (1966); T. Bowen, P. K. Caldwell, F. Ned Dikmen, E. W. Jenkins, R. M. Kalbach, D. V. Petersen, and A. E. Pifer, Phys. Rev. D 2, 2599 (1970).

[2]Particle Data Group, Phys. Lett. 50B, 1 (1974).

[3]W. Langbein, F. Wagner, Nucl. Phys. B47, 477 (1972); A. T. Lea, B. R. Martin, R. G. Moorhouse, G. C. Oades, Nucl. Phys. B56, 77 (1973); J. K. Kim, Phys. Rev. Lett. 27, 356 (1971); R. Armenteros, P. Baillon, C. Bricman, M. Ferro-Luzzi, E. Pagiola, J. O. Petersen, D. E. Plane, E. Burkhardt, H. Filthuth, E. Kluge, H. Oberlack, in *Hyperon Resonances—70*, edited by Earle C. Fowler (Moore, Durham, N.C., 1970). For a more extensive list refer to the discussion in Ref. 2.

[4]C. Daum, F. C. Erné, J. P. Lagnaux, J. C. Sens, M. Steuer, and F. Udo, Nucl. Phys. B6, 273 (1968).

[5]R. A. Arndt, R. H. Hackman, L. D. Roper, and P. H. Steinberg, Phys. Rev. Lett. 33, 987 (1974); R. Ayed, P. Bareyre, J. Feltesse, and G. Villet, Phys. Lett. 32B, 404 (1970); M. G. Albrow, S. Anderson/Almehed, B. Bošnjaković, C. Daum, F. C. Erné, Y. Kimura, J. P. Lagnaux, J. C. Sens, F. Udo, and F. Wagner, Nucl. Phys. B30, 273 (1971); S. Kato, P. Koehler, T. Novey, A. Yokosawa, and G. Burleson, Phys. Rev. Lett. 24, 615 (1970); F. Griffiths, A. Hirata, I. Hughes, D. Jacobs, R. Jennings, B. Wilson, S. Focardi, G. Giacomelli, P. Lugaresi-Serra, F. Rimondi, G. Ciapetti, G. Martellotti, D. Zanello, E. Castelli, and M. Sessa, Nucl. Phys. B38, 365 (1972); R. C. Miller, T. B. Novey, A. Yokosawa, R. E. Cutkosky, H. R. Hicks, R. L. Kelly, C. C. Shih, and G. Burleson, Nucl. Phys. B37, 401 (1972); C. Lovelace and F. Wagner, Nucl. Phys. B28, 141 (1971). For a more extensive list refer to Ref. 2.

[6]R. Odorico, Phys. Lett. 34B, 65 (1971).

[7]J. H. Goldman, Ph.D. thesis, University of Maryland Technical Report No. 73-054, 1973 (unpublished).

[8]K. Abe, B. A. Barnett, J. H. Goldman, A. T. Laasanen, P. H. Steinberg, G. J. Marmer, D. R. Moffett, and E. F. Parker, Phys. Rev. D 11, 1719 (1975).

[9]A. T. Laasanen, Ph.D. thesis, University of Maryland Technical Report No. 73-055, 1973 (unpublished).

[10]K. Abe, B. A. Barnett, J. H. Goldman, A. T. Laasanen, P. H. Steinberg, G. J. Marmer, D. R. Moffett, and E. F. Parker, Phys. Rev. D 10, 3556 (1974).

[11]K. Abe, B. A. Barnett, J. H. Goldman, A. T. Laasanen, P. H. Steinberg, G. J. Marmer, D. R. Moffett, and E. F. Parker, this issue, Phys. Rev. D 12, 1 (1975).

[12]K. Abe, Ph.D. thesis, University of Maryland Technical Report No. 73-056, 1973 (unpublished). The results reported in the present publication supersede those presented in this reference.

[13]B. A. Barnett, P. F. M. Koehler, and P. H. Steinberg, University of Maryland Technical Report No. 894, 1968 (unpublished).

[14]B. A. Leontic and J. Teiger, BNL Report No. 50031, Physics T10-4500 (unpublished).

[15]P. J. Litchfield, T. C. Bacon, I. Butterworth, J. R. Smith, E. Lesquoy, R. Strub, A. Berthon, J. Vrana, J. Meyer, E. Pauli, B. Tallini, and J. Zatz, Rutherford Laboratory Report No. RPP/H/71, 1971 (unpublished); W. P. Trower, J. R. Ficenec, R. I. Hulsizer, J. Lathrop, J. N. Snyder, and W. P. Swanson, Phys. Rev. 170, 1207 (1968); R. Crittenden, H. J. Martin, W. Kernan, L. Leipuner, A. C. Li, F. Ayer, L. Marshall, and M. L. Stevenson, Phys. Rev. Lett. 12, 429 (1964); M. Dickinson, S. Miyashita, L. Marshall Libby, and P. Kearney, Phys. Lett. 24B, 596 (1967); S. Dado, A. Birman, J. Goldberg, and H. Weiss, Phys. Rev. Lett. 29, 1695 (1972).

[16]P. Baillon, C. Bricman, M. Ferro-Luzzi, J. M. Perreau, R. D. Tripp, T. Ypsilantis, Y. Declais, and J. Seguinot, Phys. Lett. 50B, 377 (1974).